Polymer Bulletin 53, 339–347 (2005)
DOI 10.1007/s00289-005-0355-8

Polymer Bulletin

Synthesis of biodegradable PU/PEGDA IPNs having micro-separated morphology for enhanced blood compatibility

Sung-Soo Yoon[1], Jong-Hun Kim[2], Sung-Chul Kim[1](✉)

[1]Center for Advanced Functional Polymers, Department of Chemical and Biomolecular Engineering, Korea Advanced Institute of Science and Technology, 373-1, Guseong-dong, Yuseong-gu, Daejeon 305-701, Korea
[2]Chemicals & Polymers Research and Development, LG Chemicals Ltd., P.O.Box 61 Yu Sung, Science Town, Daejeon 305-380, Korea

E-mail: kimsc@kaist.ac.kr, Fax: +82-42-869-8435

Received: 26 November 2004 / Revised version: 23 January 2005 / Accepted: 13 February 2005
Published online: 24 February 2005 –

Summary

New biodegradable hydrophobic polyurethane (PU) / hydrophilic poly (ethylene glycol) diacrylate (PEGDA) IPN was simultaneously synthesized with changing the molecular weight of PEGDA to investigate the effect of crosslinking density on the degree of phase separation. PU was modified using biodegradable poly(ε -caprolactone)diol and the hydroxy group of PEG was substituted to crosslinkable acrylate group having double bond, which induce photo-polymerization. The sturucture of PEGDA was confirmed by NMR. Because the reaction rate of PEGDA was faster than that of PU, the continuous matrix of the micro-separated PU/PEGDA IPNs having amphiphilic character was made of hydrophilic PEGDA-rich phase. All IPNs have sea-island morphology resulting from the suppressed phase separation. The effect of the degree of phase separation on blood compatibility was investigated.

Introduction

Biocompatibility , especially blood compatibility, is an important issue because biomaterials implanted in human body must perform without disturbing biological system [1]. It was reported that blood compatibility is mainly influenced by the surface properties such as morphology, roughness, hydrophilicity, etc [2-7]. In our early studies, hydrophilic PU/hydrophilic PU IPNs exhibited good blood compatibility as well as excellent mechanical properties. We also investigated the effect of the degree of phase separation on blood compatibility. The reaction temperature, composition of monomers, and the crosslink density, significantly affected the blood-compatibility since the size of the dispersed PS-domain was affected by those conditions [8-10]. The effect of PEO pendent chain on surface morphology and blood compatibility was also investigated [11-12]. As a result, IPNs with micro-separated structure showed excellent blood compatibility in the short-term blood test. However, as most synthetic biomaterials, the hydrophilic PU / hydrophobic PS IPNs might have

problems in long-term clinical use. In the present study, polyurethane was modified using biocompatible and biodegradable PCL diol and the hydroxyl group of PEG, which has widely been known for good biocompatibility, was substituted by crosslinkable acrylate group [13-17]. Then new biodegradable hydrophobic polyurethane(PU)/hydrophilic poly(ethylene glycol)diacrylate (PEGDA) IPNs were synthesized to investigate the effect of molecular weight of PEGDA on the surface morphology and blood compatibility.

Experimental

Materials

Poly(ethylene glycol)s (PEG) with molecular weights of 2000 g/mol, 4000 g/mol, 6000 g/mol were purchased from Fluka company Inc. Poly(ε -caprolactone) diol (PCL, Mn = 530 g/mol, Aldrich Chemical Company Inc.), 1,4-butanediol(1,4-BD, Junsei Chemical Co., Ltd) and trimethylolpropane (TMP, Acros Organics) were also degassed at 65^{o}C for 12h under vacuum to remove moisture before use. Hexamethylene diisocyanate (HDI, Tokyo Kasei Kogyo Co., Ltd.), acrylolyl chloride (Aldrich Chemical Company Inc.), triethylamine (TEA, Acros Organics, anhydrous), benzene (Aldrich Chemical Company Inc.) were used without purification. Benzoin (Aldrich Chemical Company Inc.) was used as the photoinitiator.

Synthesis of PEGDA and PU/PEGDA IPNs

Crosslinkable PEGDA was prepared by substituting the hydroxyl end group of PEG by acrylate group [13]. Acrylolyl chloride dissolved in benzene, in three fold molar excess based on hydroxyl groups of PEG, was dropped to the PEG solution having TEA at room temperature. The reaction proceeded overnight at 35^{o}C under nitrogen. After removing triethylamine hydrochloride salt, the filtrate was precipitated in n-hexane twice. The precipitated PEGDA was dried at 40^{o}C for 24h under vacuum.
Diisocyanate-terminated PU prepolymer was prepared by reacting 1 equiv. of poly(ε -caprolactone) diol with 2 equiv. of HDI at 65^{o}C for 2h under nitrogen. 0.05 wt% dibutyltindiaurate (T-12) as a catalyst was added to poly(ε -caprolactone) diol before reaction. HDI was charged into a four-necked flask and was heated at 65^{o}C and then the degassed poly(ε -caprolactone) diol was added dropwise to HDI. The completeness of the reaction was identified by the di-n-butylamine titration method [18]. PU networks were prepared by reacting the diisocyanate-terminated PU prepolymer with 1,4-BD as a chain extender and TMP as a crosslinking agent. 1,4-BD and TMP were mixed and degassed before reaction. The equivalent ratio of 1,4-BD and TMP to isocyanate was respectively to give theoretical $\overline{Mc}$ (=1910). PU/PEGDA IPNs having various domain sizes were prepared by changing the molecular weight of PEGDA. After mixing PU prepolymer, 1,4-BD, TMP, PEGDA and benzoin (fixed at 1wt% based on PEGDA weight), the homogeneous mixture was cast in a glass plate mold with a silicon spacer and the PU network and PEGDA network were formed simultaneously in UV chamber at 80^{o}C for 5h. PEGDA network was formed by exposing the mixture under UV (max. wavelength = 350nm). The weight fraction of PEGDA and PU in PU/PEGDA IPNs was 50wt%.

NMR and DSC

The structure of the synthesized PEGDA was confirmed by ^{1}H-NMR that were recorded by Bruker AMZ 500 spectrometer with $CDCl_3$-d (Aldrich) solvent. The thermal property of synthesized PU network, PEGDA networks and PU/PEGDA IPNs were studied by using differential scanning calorimeter (DSC, Q500, TA instrument). The heating rate was 10^{o}C/min. The mid-point of the step change in heat capacity was determined as the glass transition temperature (Tg).

Reaction Kinetics

The conversion of the double bond in acrylate group in the formation of PEGDA network was investigated by using FT-IR equipped with demountable liquid cell having NaCl window. During the polymerization, samples were taken out from the UV-chamber at pre-determined time intervals. Conversion was determined by measuring the ratio of carbonyl peak intensity (at 1720 cm^{-1}) to double bond peak intensity (at 1625 cm^{-1}). Conversion of isocyanate group during the formation of the PU network was also investigated by FT-IR equipped with demountable liquid cell, and heating accessory. Conversion of was determined by observing the decrease of isocyanate peak area (at 2271 cm^{-1}), caused by the formation of the urethane linkage.

Morphology

The morphology of the top surface of the PU/PEGDA IPNs was investigated by the scanning probe microscopy (SPM, DI NanoScope IIIa). SPM measurement was performed in air with an etched silicon probe, of which the length was 125 μm, and the spring constant was from 20 to 100 N/m. Scanning was carried out in the Tapping^{TM} mode, and its frequency was about 0.5 Hz. In this study, the surface morphology of PU/PEGDA IPNs under water was also observed by using SPM equipped with the oxide-sharpened tip, and liquid-tip-holder. PU/PEGDA IPNs were equilibrated with distilled water before the experiment. Scanning was carried out in the Tapping^{TM} mode, and its frequency was about 0.5 Hz.

Interfacial Energy

Interfacial energy between the surfaces of PU/PEGDA IPNs, PU network, PEGDA networks and water was measured by an underwater captive bubble technique. The samples were equilibrated with distilled water for more than 24 hours, and the static bubble contact angles of the surface-water-air and the surface-water-octane were then measured by a contact angle goniometer (Erma model G-I type) equipped with an oil droplet apparatus in the water. Interfacial energy between the surface and the water was calculated from the harmonic mean equation [19-20].

$$\gamma_{12} = \gamma_1 + \gamma_2 - 4\left(\frac{\gamma_1^d \gamma_2^d}{\gamma_1^d + \gamma_2^d}\right) - 4\left(\frac{\gamma_1^p \gamma_2^p}{\gamma_1^p + \gamma_2^p}\right)$$

In vitro Platelet Adhesion Test

After samples (10×10 mm^2) were equilibrated with PBS overnight, they were then immersed in platelet rich plasma (PRP), which was obtained from white rabbit, at

37 ^{o}C with mild shaking in an incubator. After ten hours, the samples were taken out from the solution and rinsed five times with PBS to remove the weakly adsorbed platelets. After fixing the strongly adsorbed platelets using 2-v/v% glutaraldehyde for 2 hours, the samples were dehydrated with a series of ethanol solutions (50, 60, 70, 80, 90, 100 v/v%) for 15 min per each step. Then they were dried in atmosphere overnight and under vacuum for five hours. Then, the adherent platelets were observed with SEM [21]. In addition, PU/ PEGDA IPN films were attached on Petri dishes (surface area: 660 mm^2) by using a silicone adhesive, and then contacted with 2 ml of PRP previously prepared (2×10^7 cells/ml) at 37 ^{o}C with mild shaking in an incubator. After 10-hours incubation, the number of the not-adhered platelets was measured by using a hemacytometer, and the %-adhesion and the number of platelets adhered were calculated.

Results and Discussion

The upper spectrum of Figure 1 a) is that of PEG 2k and the lower spectra is that of PEGDA 2k. New peaks (5.8, 6.1 and 6.4 ppm), which were not shown in the PEG 2k, appeared due to the acrylate group of PEGDA 2k. In particular, these three peaks show the triplet. The peak around 4.3ppm was that of the ethylene group of PEG backbone adjacent to the acrylate group. This peak was shifted from 3.7ppm to 4.3ppm due to the acrylate group. From Figure 1 b), c), the same results were shown for PEGDA 4k and PEGDA 6k. The acrylate peak intensity of PEGDA was decreased with increasing the molecular weight of PEG due to the reduced concentration of the end functional group. Due to the appearance of these three peaks, it was confirmed that the end hydroxyl group of PEG was substituted to acrylate group. The degree of substitution of the end hydroxyl group of PEG for acrylate group was about 100% in all PEGDA using the method of Dust et al [22]. Consequently, the hydroxyl group of PEG was successfully substituted by the acrylate group. The Tg of PEGDA2k network was – 48.8^{o}C and the Tg of PEGDA part of PU/PEGDA2k IPN was – 43.9^{o}C showing the Tg shift about 5^{o}C. The Tg of PU/PEGDA 4k, 6k IPN also show Tg shift

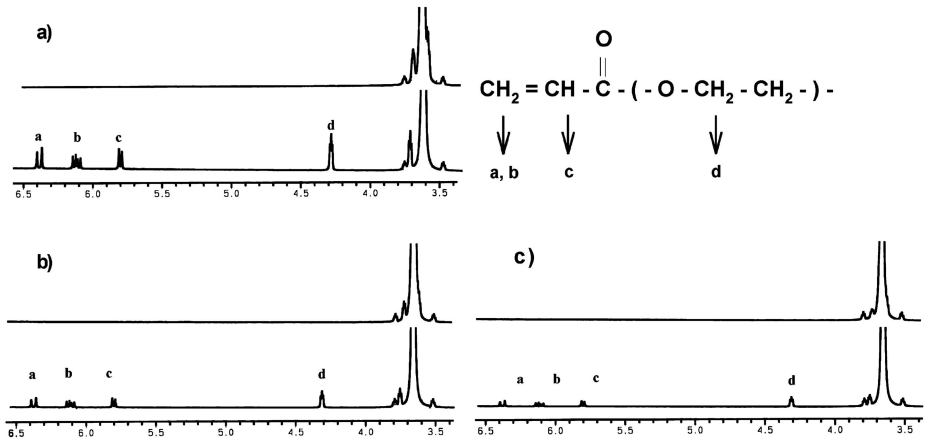

Figure 1. NMR spectrum of PEG and PEGDA: a) PEG 2k and PEGDA2k b) PEG 4k and PEGDA 4k c) PEG 6k and PEGDA 6k

of 5-6°C in the PEGDA Tg. The Tg of PU homo network is about –20.2°C. But in PU/PEGDA IPNs, the Tg of PU part was not clearly observed. The Tg of PEGDA networks decreased with increasing the molecular weight of PEG due to the decreased crosslinking density (figure not shown). This trend was also shown in PU/PEGDA IPNs. In the formation of PU network, the isocyanate peak at 2271 wavenumber(cm^{-1}) of PU gradually decreased and finally disappeared as the reaction was proceeded.
The reaction of PU reached the equilibrium state after about 3 hours. The double bond peak of PEGDA decreased as the reaction proceeded. The reaction kinetics of PEGDA was investigated by measuring the peak area ratio between the carbonyl group and the double bond group. The reaction of PEGDA reached the equilibrium faster than PU. Due to the faster formation of PEGDA network than PU, the PEGDA-rich phase formed the continuous matrix and the PU-rich phase formed the dispersed domain. In PEGDA 2k network, 73.6 % of double bond was incorporated in the formation of PEGDA network. In PEGDA 4k, 6k, 76.7%, 70.4% of double bond was incorporated in the reaction.

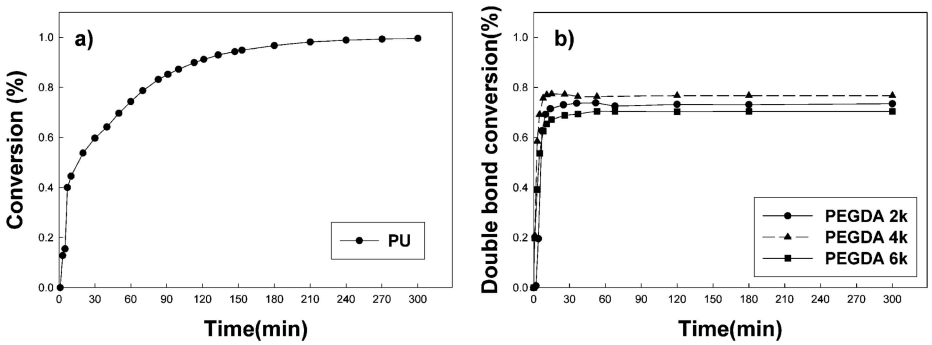

Figure 2. Kinetics of polymerization ; a) PU synthesis b) PEGDA synthesis

The gel content of PEGDA 2k homo network was 98.3% and those of PEGDA 4k, 6k home networks were 98.7%, 98.5% respectively. All PU/PEGDA IPNs show above 99.5% gel content. These high gel content implies that almost all of the PEG chain with unreacted terminal acrylate group was grafted to the main chain. As the PEGDA forms crosslinked network, the Tm and the heat of fusion decreased when compared to PEGDA macromonomer, which was shown in Table 1, and the decrease became smaller as the PEG molecular weight was increased with lower crosslink density. Since the hydrophilic PEGDA network was formed faster than the hydrophobic PU network, the continuous matrix was the hydrophilic PEGDA-rich phase and the dispersed domain was the hydrophobic PU-rich phase. In PU/PEGDA 2k, 4k IPNs,

Table 1. T_m and heat of fusion of PEGDA and PEGDA networks

	T_m (°C)	ΔH_m (J/g)
PEGDA 2k	53.7	148.4
PEGDA 2k network	19	40.4
PEGDA 4k	59.6	149
PEGDA 4k network	39.8	60.5
PEGDA 6k	61.3	150.4
PEGDA 6k network	44.3	65.2

the surface morphology were sea-island morphology, but in PU/PEGDA 6k IPN, the sea-island morphology having some co-continuity was shown. The average diameter of the PU-rich phase was decreased from 47nm to 11nm, as the molecular weight of PEGDA was decreased. Namely the domain size of the PU-rich phase decreased as the crosslinking density of PEGDA network was increased. The morphology of the surfaces of PU/PEGDA IPNs in water is also shown in Figure 3. The morphology of PU/PEGDA IPNs in water shows also microphase-separated sea-and-island morphology, same as in air, which indicated that the microphase-separated structure was very stable in water and the morphological rearrangement at the water-polymer interface was prohibited by the interlocking between the PU- rich and the PEGDA-rich phases of PU/PEGDA IPNs. The average diameter of the PU-rich phase also decreased, as the molecular weight of PEGDA decreased due to the increased crosslinking density. This trend was the same as the case in air. The average diameter of the PU-rich phase of the PU/PEGDA 6k IPN was 45nm, which was the largest domain size in all PU/PEGDA IPNs. With decreasing the PEG molecular weight the phase separation of PU/PEGDA IPNs was suppressed to result in small hydrophobic domains in sizes around 17 nm.

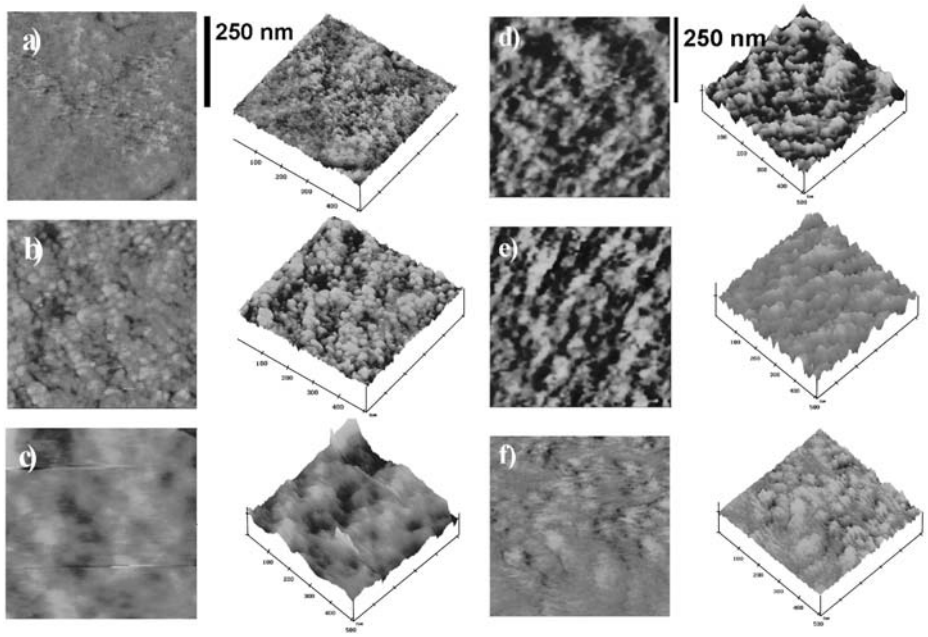

Figure 3. The surface morphology of PU/PEGDA IPNs; in air a) PU/PEGDA 2k IPN b) PU/PEGDA 4k IPN c) PU/PEGDA 6k IPN ; in water d) PU/PEGDA 2k IPN e) PU/PEGDA 4k IPN f) PU/PEGDA 6k IPN

Interfacial energy between PU/PEGDA IPNs, PU homo network, PEGDA homo networks and water was listed in Table 2. Whereas interfacial energy of PU network with water was 18.7 dyne/cm, that of PEGDA 2k, 4k, 6k network were respectively 4.8, 3.9, 1.9 dyne/cm. The interfacial energy of PU/PEGDA IPN was varied from 8.2 dyne/cm to 6.1 dyne/cm, which was between that of PU network and that of PEGDA network. As a result, the interfacial energy of PU/PEGDA IPN and PEGDA network

with water decreased with increasing the molecular weight of PEGDA, that is, the surface hydrophilicity increased as increasing PEGDA molecular weight.

Table 2. Interfacial energy of PEGDA networks, PU network and PU/PEGDA IPNs with water

	Surface-water-air (degree)	Surface-water-octane (degree)	γ_{sw} (dyne/cm)
PEGDA2K Network	37.3 ± 1.5	54.6 ± 1.7	4.8 ± 0.9
PEGDA4K Network	35.1 ± 2.3	53.1 ± 0.7	3.9 ± 0.9
PEGDA6K Network	31.8 ± 1.6	49.3 ± 1.2	1.9 ± 0.6
PU Network	59.0 ± 1.4	72.7 ± 1.2	18.7 ± 1.1
PU/PEGDA2K IPN	53.8 ± 2.1	69.0 ± 1.0	8.2 ± 0.4
PU/PEGDA4K IPN	48.6 ± 2.1	63.6 ± 1.1	6.5 ± 0.5

Surface properties of biomedical polymers govern the blood compatibility of them, and especially, surface morphology and surface energy are key factors determining antithrombogenicity of the materials. Whereas highly hydrophilic surface as well as highly hydrophobic surface does not have good antithrombogenesis, the balanced surface having amphiliphiic character has good antithrombogenesis. In this study, we focused on the effect of micro-separated surface morphology on platelet adhesion. Platelets have a very important role in hemostasis and thrombogenesis. Platelets initially arrest bleeding through formation of platelet plugs, and stabilize platelet plugs by catalyzing the coagulation reaction, leading to the formation of fibrin though there is no special interaction with other blood cells. In this study, the interaction of platelets with the surfaces of PU homo network, and PU/PEGDA IPNs was investigated by using platelet rich plasma (PRP) prepared from white rabbit whole

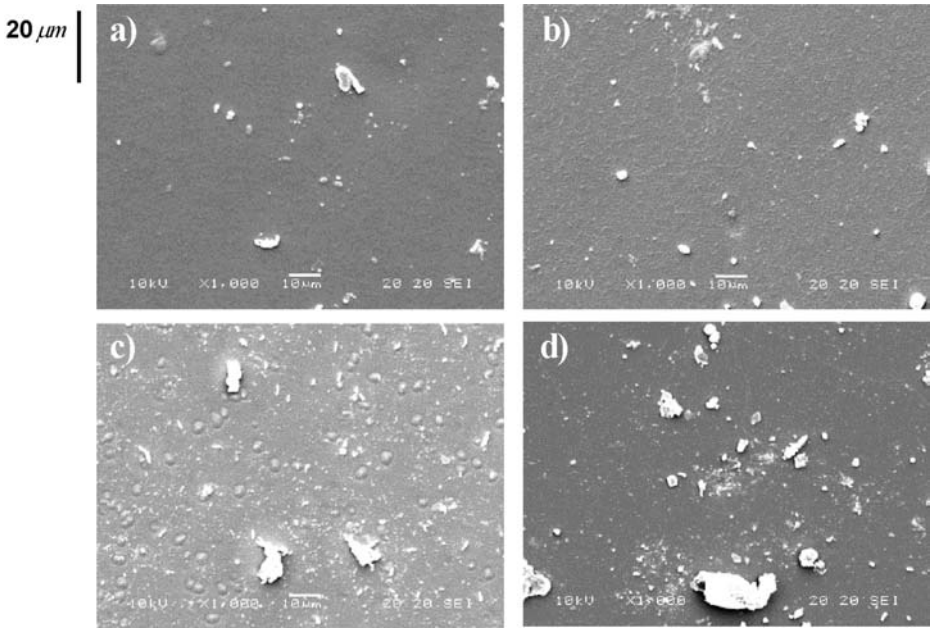

Figure 4. SEM image of adhered platelet on the surface: a) PU/PEGDA 2k IPN b) PU/PEGDA 4k IPN c) PU/PEGDA 6k IPN d) PU network

blood. In all IPNs, the mural thrombosis, which means the aggregation of the platelets, was not observed, while in PU network, aggregation was observed. On the PU/PEGDA IPNs, the expression of the platelet glycoproteins was suppressed by regulating the excessive assembly of the proteins. This means that the second thrombosis was suppressed by the micro-separated structure of the PU/PEGDA IPNs. The number of adhered platelets on PU homo network was 66464 mm^{-2}, which was relatively higher than those of PU/PEGDA IPNs due to the effect of micro-separated structure of IPN on suppression the platelet adhesion. In PU/PEGDA IPNs, the number of adhered platelets was decreased from 59057 mm^{-2} to 38181 mm^{-2} with decreased hydrophobic domain size due to the suppressed phase separation.

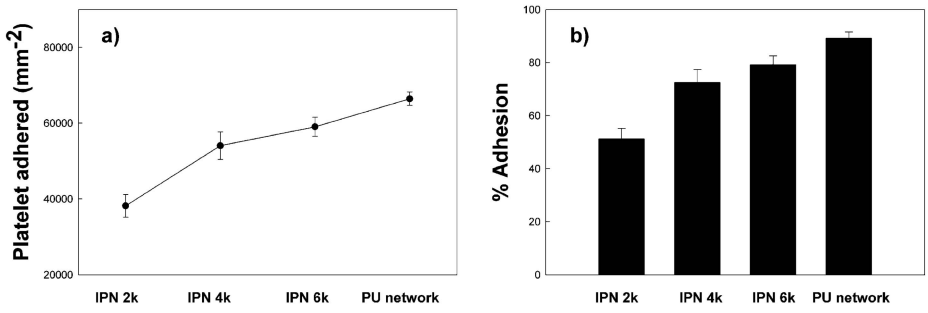

Figure 5. a) The number of platelet adhered on PU/PEGDA IPNs and PU network, b) % adhesion of platelet on PU/PEGDA IPNs and PU network

Conclusion

PU/PEGDA IPNs were synthesized changing the molecular weight of PEGDA. From the DSC results, it was shown that all PU/PEGDA IPNs had one broad Tg between the Tgs of two pure components. All PU/PEGDA IPNs had micro-separated structure in which the PEGDA-rich phase formed the continuous matrix and the PU-rich phase formed the dispersed domain, since the reaction rate of PEGDA was faster than that of PU. The domain size of PU/PEGDA IPNs decreased as decreasing the molecular weight of PEGDA, which indicated an increase in the intermixing between the PU-rich phase and the PS-rich phase. The micro-separated structure was stable in water and the domain size was almost the same as air. The amount of adhered platelet of all PU/PEGDA IPNs was lower than that of PU homo network due to the micro-separated structure of IPN. In PU/PEGDA 2k IPN, relatively smaller amount of platelet was adhered due to the smallest hydrophobic domain size of the surface morphology in all PU/PEGDA IPNs. Therefore, the blood compatibility of PU/PEGDA IPNs was enhanced by decreasing the molecular weight of PEGDA due to the increased crosslinking density of the PEGDA network.

References

1. Ratner BD, Hoffman AS (1996) Biomaterials Science; An introduction to materials in Medicine. Academic Press, New York
2. Okano T, Akaike T, Kataoka K, Tsuruta T (1981) J Biomed Mater Res 15:393
3. Takahara A, Tashita J, Kajiyama T, Takayanagi M, MacKnight WJ (1985) Polymer 26:978

4. Takahara A, Tashita J, Kajiyama T, MacKnight WJ (1985) Polymer 26:987
5. Okano T, Kikuchi A, Sakurai Y, Takei Y, Ogata N (1995) J Controll Release 36:125
6. Blezer R, Lindhout T, Keszler B, Kennedy JP (1995) Polym Bull 34:101
7. Bahulekar R, Tamura N, Ito S, Kodama M (1999) Biomaterials 20:357
8. Shin YC, Han DK, Kim YH, Kim SC (1994) J Biomater Sci Polym Edn 6:195
9. Shin YC, Han DK, Kim YH, Kim SC (1994) J Biomater Sci Polym Edn 6:281
10. Roh HW, Song MJ, Han DK, Lee DS, Ahn JH, Kim SC (1999) J Biomater Sci Polym Edn 10:123
11. Kim JH, Kim SC (2003) Macromolecules 36:2867
12. Kim JH, Kim SC (2002) Biomaterials 23:2015
13. Sawney AS, Pathak CP, Hubbel JA (1993) Macromolecules 26:581
14. Jo SB, Shin HS, Shung AK, Fisher JP, Mikos AG (2001) Macromolecules 34:2839
15. Ju YM, Ahn KD, Kim JM, Hubbell JA, Han DK (2003) Polym Bull 50:107
16. Padmavathi NC, Chatterji PR (1996) Macromolecules 29:1976
17. Malucelli G, Sangermani M, Bongiovanni R, Priola A, Keddie Jl (2000) Polym. Bull 45:431
18. Hepburn C (1955) Polyurethane Elastomers 2nd Ed. Elsevier, New York
19. Andrade JD, Ma SM, King RN, Gregonis DE (1979) J colloid and interface Science 72:488
20. Schrader ME, Loeb GI (1992) Modern Approaches to wettability. Plenum Press, New York
21. Han DK, Jeong SY, Kim YH (1989) J Biomed Mater Res Appl Biomater 23:211
22. Dust JM, Fang Z, J. Harris M (1990) Macromolecules 23:3743